

IFIRS: An Imaging Fourier Transform Spectrometer for the Next Generation Space Telescope

James. R. Graham

Department of Astronomy, University of California, Berkeley, CA 94720

Abstract.

Due to its simultaneous deep imaging and integral field spectroscopic capability, an Imaging Fourier Transform Spectrograph (IFTS) is ideally suited to the Next Generation Space Telescope (NGST) mission, and offers opportunities for tremendous scientific return in many fields of astrophysical inquiry. We describe the operation and quantify the advantages of an IFTS for space applications. The conceptual design of the Integral Field Infrared Spectrograph (IFIRS) is a wide field ($5'.3 \times 5'.3$) four-port imaging Michelson interferometer.

1. Introduction

IFIRS is a Michelson interferometer configured as an imaging Fourier transform spectrometer (IFTS) (Graham et al. 1998; Graham et al. 2000). Fig. 1 shows a moving mirror which introduces an optical path difference (OPD) between the two beams created by the beam-splitter; the resulting interferogram from the combined beams is recorded for every pixel in the field of view, and hence a spectrum is obtained for every object. Since the bandpass of the instrument is defined only by the detectors and the efficiency of the beam-splitter, broad wavelength coverage is an intrinsic feature of the IFTS. An IFTS has continuously variable spectral resolution up to a maximum defined by the maximum OPD, which in the IFIRS design is 1 cm (i.e., $R_{max} = 10,000$ at $1 \mu\text{m}$). IFIRS is a four-port interferometer, a choice which yields several advantages. (1) Virtually all the light collected by the telescope is directed toward the focal plane for detection. (2) The final interferogram, constructed from the difference of the two output ports, is immune to common mode noise.

When the interferograms from the two output ports are summed, the total flux image is recovered, producing the simultaneous deep panchromatic image that is a unique capability of an IFTS. In comparison with a simple camera, in which the panchromatic image is formed by summing individual filter images, the IFTS panchromatic image has a speed advantage factor equal to the number of filters used. In its hybrid, or dispersed FTS mode, designed for use with slit masks at high spectral resolution ($R \simeq 600-10,000$), IFIRS delivers a sensitivity for each object equivalent to that of a conventional dispersive spectrograph, with the spatial multiplex advantage of a multi-object spectrometer. The capabilities of IFIRS are summarized in Table 1.

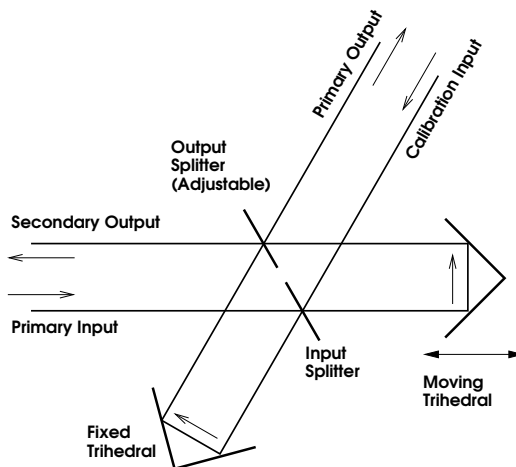


Figure 1. An IFIRS is a Michelson interferometer where the telescope focal plane is imaged onto a detector array. An interferogram is recorded for every pixel, and hence a spectrum can be obtained for every object. IFIRS has a four-port design that wastes none of the light. IFIRS uses cube-corners, which displace the input and output beams.

Table 1. **Observational Capabilities of IFIRS**

	Near-IR Channel	Mid-IR Channel
Bandpass/Detector	0.6-5.6 μm /InSb	3-28 μm /Si:As
Maximum Spectral Resolution, R	15,000	3000
FOV/Array Format	5.'3/8k \times 8k	2.'6/2k \times 2k
Pixel size/Nyquist sampled λ	0.''0386/3 μm	0.''0772/6 μm
Wavefront error/Strehl	150 nm rms/0.8	150 nm rms/0.99
Throughput (excluding detector)	86%	87%
FTS Sensitivity, $R = 1/5/100$	0.2/1/35 nJy	13/65/1300 nJy
Dispersed FTS Sensitivity, $R = 600$	66 nJy	1080 nJy

Strehl ratios and sensitivities are quoted at 2 & 10 μm . $SNR = 10$, $t = 10^5$ s.

2. IFIRS Performance

Since NGST must obtain images and spectra of large samples of objects in order to achieve its science goals, IFIRS's ability to deliver diffraction-limited full-field imaging spectroscopy is a critical advantage. Fig. 2 compares the noise equivalent flux density (NEFD) per pixel as a function of spectral resolution for NGST backgrounds at 2 μm for a tunable filter camera, a dispersive spectrometer, and an IFTS (Bennett 2000). The IFTS substantially outperforms both the tunable filter and the dispersive spectrometer used in mapping mode. The dispersive spectrometer has the best performance for spectroscopy, although only for the small number of objects that lie on the slit.

A hybrid approach (e.g., Beer 1992), which takes advantage of the best features of all of the 3-d imaging approaches, is the combination of an objective prism with an IFTS. Low dispersion in one dimension of the image plane reduces the spectral bandpass acceptance that is involved in the noise term for the IFTS.

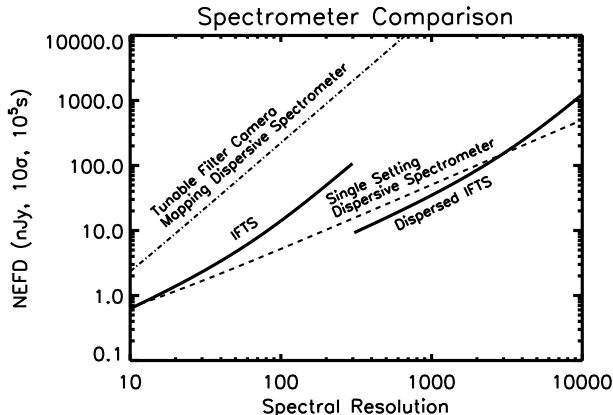


Figure 2. The NEFD per pixel for a variety of NGST imaging spectrometers (Bennett 2000). All observations extend over the K -band. The IFTS obtains spectra for every pixel. For $R > 300$ the IFTS curve is for the dispersed IFTS mode. The mapping dispersive spectrometer is scanned over a number field of view settings, assumed to be equal to the number of spectral channels acquired by the tunable filter camera, and thus they have equal NEFD. The single setting dispersive spectrometer acquires spectra for a single pointing. The same NEFD level is achieved by a tunable filter camera if all the integration time is devoted to observing a single wavelength.

With a slit at an image plane, the panchromatic output of the IFTS would yield the same results as an ordinary prism spectrometer, while the Fourier transformed interferograms would enable much higher spectral resolution at much reduced NEFD. The $R > 300$ segment of the FTS curve in Fig. 2 is for this hybrid configuration, and corresponds to the addition of an $R \simeq 600$ dispersing prism and a focal plane mask.

The curves in Fig. 2 depend on detector performance. Detectors with higher read noise and dark current would decrease the sensitivity of the tunable filter, the dispersive spectrometer, and the dispersed IFTS, but produce little change in the IFTS.

One important aspect of the IFTS is that the sensitivity to an unresolved line is independent of R , so long as read noise can be neglected. Fig. 3 illustrates this by showing the same star forming galaxy at $R = 100$ and 1000. In each case $\text{Ly}\alpha$ is detected with the same SNR. In a FTS the noise is determined by the total photon shot noise, i.e., it depends only on the total integration time. Therefore, so long as the line is unresolved, the SNR remains constant. The same is true for a dispersive spectrometer which is dark current limited, which is typically the case for NGST. In the dark current limited domain the dispersive spectrometer loses much of its advantage for high spectral resolution observations.

2.1. Spectrometer Comparisons

Several programs in the NGST design reference mission (DRM) call for low resolution spectra of large numbers of faint ($K > 29$ AB) objects. Since dispersive spectrometers on NGST are dark current limited, they are unsuitable for large

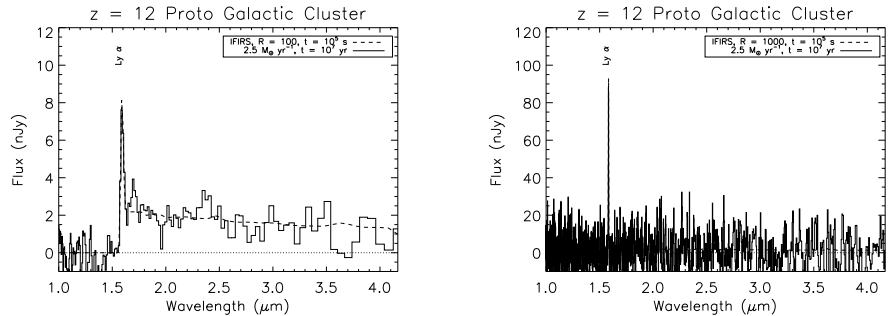


Figure 3. The sensitivity of an pure IFITS is independent of spectral resolution. Simulated observations of a $z = 12$ star forming cluster are shown at $R = 100$ and $R = 1000$. The exposure time is fixed. Low or high resolution IFITS scans can be used to search for line emission, or broad spectral features such as the Lyman break. Kinematics, chemical composition, or peculiar velocities can be measured in the same exposure time at high resolution.

sample surveys. Survey science is crucial to NGST; for example, one component of the galaxy evolution DRM consists of validating photometric redshifts with $R \simeq 100$ spectroscopy. The accuracy and precision of photometric redshifts should be investigated over a range of galaxy properties. Since statistical errors scale as the square root of the number of galaxies in each bin, of order 100 galaxies are needed per bin. Without such large numbers multiplicative factors decimate small samples to statistical meaninglessness. A modest sample to test photometric redshifts consists of 10-redshift \times 5-luminosity \times 2-color \times 3-environment \times 3-morphology bins \times 100 galaxies per bin = 90,000 galaxies. The IFITS can perform a complete magnitude limited sample to $K = 29$ AB in three days. An MOS would take 45 days to complete this survey.

To discover and characterize the population of sources which reionize the universe at $z \gtrsim 10$ requires winnowing out sources which comprise $< 0.1\%$ of the population at $K \simeq 29 - 30$ AB (Haiman & Loeb 1998). Clearly thousands of spectra are needed for this task to: 1) find the high- z population; 2) distinguish AGN from objects powered by star formation. Once these distant star-clusters, galaxies, or quasars have been identified, their spectra may be coadded to construct a very high signal-to-noise ratio composite spectrum that is a sensitive probe of the re-ionization epoch. Rather than hoping to find a single bright target in the dark ages, composite coadded spectra may be the most reliable way to search for the reionization epoch: the luminosities and masses of the first collapsed objects are unknown, and there are likely to be many more small (faint) ones than large (bright) ones.

These science programs suggest that it is appropriate to define the figure of merit used to compare a MOS and an IFITS as the ratio of the number of galaxy spectra obtained. We assume that a magnitude limited catalog is obtained in a fixed observing time, and the same wavelength range and number of spectral channels for each instrument.

For a single object a dispersive spectrometer is faster than the IFITS by a factor which is proportional to R , under the assumption of photon shot noise limited performance. Thus, if the integral galaxy number counts scale as $f_0^{-\alpha}$,

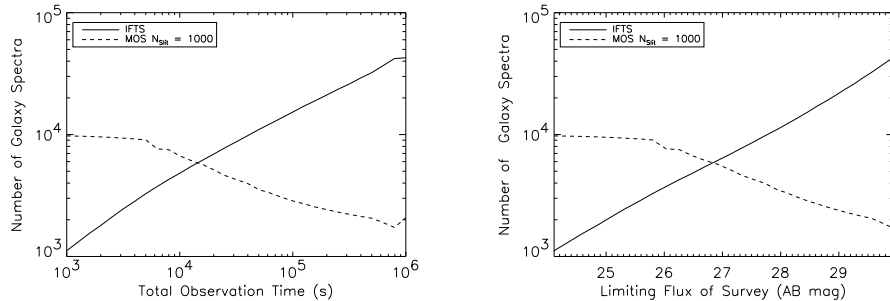


Figure 4. Comparison of number of galaxy spectra ($SNR > 10$) obtained as a function of the limiting magnitude and total observation time for a multislit dispersive spectrometer and an IFTS. The parameters are: IFTS FOV = $5' \times 5'$; $N_{slit} = 1000$; $R = 100$; $\Delta\lambda = 1.3 - 2.6 \mu\text{m}$ (FSR of a $2 \mu\text{m}$ blazed grating, $m = 1$); dark current: $0.02 e^- s^{-1}$; read noise: $4.0 e^- \text{rms}$; maximum time before readout to veto cosmic rays: 800 s.

then the speed of the IFTS compared to a MOS is proportional $f_0^{-\alpha}/(N_{slit}R)$ where f_0 corresponds to the magnitude limit of the catalog and N_{slit} is the number of MOS slits (assuming one object per slit). At faint enough fluxes the IFTS always wins because the predicted value of $\alpha \simeq 1$ (Haiman & Loeb 1998). The conclusion is strengthened because dispersive spectrometers on NGST tend to be dark current limited. The MOS enters the domain of diminishing returns for targets where dark current dominates the noise

Fig. 4 shows the results of a more realistic comparison which plots the total number of galaxy spectra obtained in a survey. The IFTS observation is done by using the integration time to observe one field. For bright objects, the MOS has the speed to observe multiple fields. Thus the number of MOS spectra equals N_{slit} times the number of pointings. The surface density of galaxies is derived from the Haiman & Loeb (1998) and Im & Stockman simulations and normalized to deep NICMOS counts (Fig. 5). The two plots which make up Fig. 4 are projections of a single 2-d surface which describes the results of the observation. Either the total observation time or the limiting magnitude of the survey can be considered as the independent variable.

For $K < 26$ AB the MOS is photon shot noise limited, and is a fixed factor faster than the IFTS. The MOS can take data for $\simeq 10$ pointings and obtain spectra for $\simeq 10,000$ galaxies. Because such faint galaxies are rare, the IFTS can only obtain spectra for a few thousand galaxies within its FOV. For $K > 26$ AB the MOS is dark current limited, and the speed advantage relative to the IFTS declines. By $K = 26.9$ AB the MOS and the IFTS acquire equal numbers of galaxies. As we enter the domain of scientific interest to NGST, $K > 28$ AB, the IFTS obtains an order of magnitude more galaxy spectra than the MOS. Fig. 4 shows that the only practical way to complete the two examples of low resolution spectroscopy from the DRM is with an IFTS.

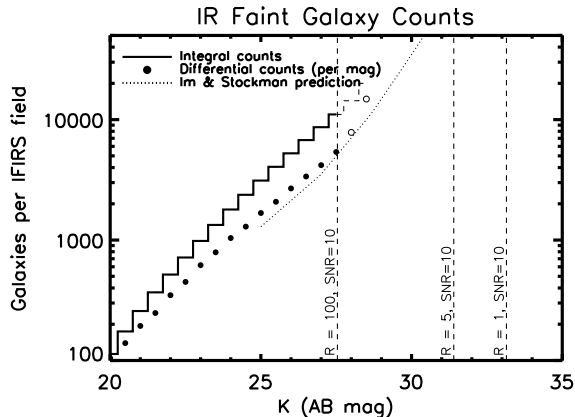


Figure 5. Merged galaxy counts from Yan et al. (1998) for $H < 25.9$ AB, Bershady et al. (1998) for $K < 24.9$ AB, Thompson et al (1999) for $H < 28.8$ AB. Incompleteness has been corrected according to Thompson et al. For $K > 27.5$ AB a dashed line or open symbols indicate where uncertainties are significant ($\gtrsim \times 2$) due to small field observed by NICMOS, photometric errors, and statistical errors. The IFIRS $SNR = 10$ thresholds for deep exposures (10^5 s) at $R = 1, 5,$ & 100 at K are indicated by the vertical lines.

3. IFIRS Science

This brief note only permits description of a few of the NGST science programs that benefit from an FTS architecture.

The Origin and Evolution of Galaxies: A cornerstone of NGST’s science is to understand the formation and evolution of galaxies. NGST is uniquely positioned to investigate the formation of the first galaxy fragments, their growth by merging into galaxies, and the subsequent chemical and dynamical evolution into the present day Hubble sequence. These science goals are addressed by five conventional imaging and spectroscopic surveys in the DRM. The surveys target relatively large samples of galaxies: imaging is required to determine morphology and select spectroscopic samples, low resolution $R \simeq 100$ spectroscopy of large samples targets global properties (e.g., redshifts, star formation rate, metallicity, mean stellar age), and higher resolution $R \simeq 1000$ spectroscopy of smaller samples to determine gas phase abundance, stellar content, dynamical masses, and dust content.

The steeply rising galaxy number counts (Fig. 5) suggest that the NGST focal plane may be crowded with $\sim 10^5$ faint galaxies per 5.3×5.3 FOV, i.e., one object per square arcsecond. The efficient study of objects at high surface densities necessitates a highly multiplexed approach, such as that afforded by IFIRS. IFIRS’s ability to simultaneously carry out the imaging and low spectral resolution studies increases efficiency by combining different science programs in a single observation and enhances the discovery potential.

To demonstrate the ability of IFIRS to detect and study faint objects we have simulated data as follows. An astronomical scene is represented as a noise-free distribution of objects and associated spectra. This input data cube is

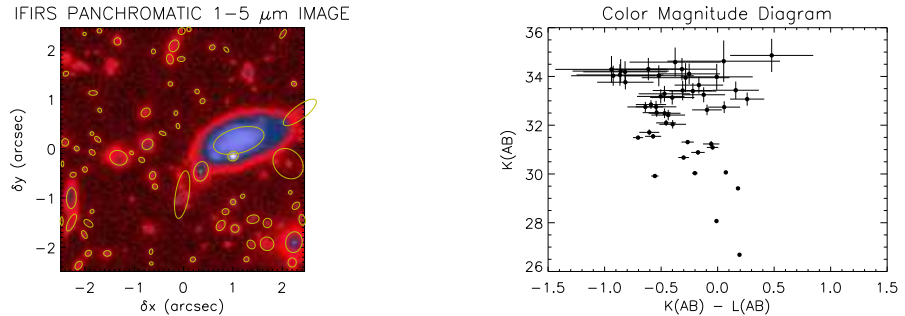


Figure 6. Simulated ultra-deep (10^6 s) *ZJHKLM* observations. This region corresponds to 0.02% of the IFIRS field of view and contains a $K = 26.0$ AB, $z = 4.67$ spiral and 60 $z > 5$ star-forming galaxies brighter than $K \approx 33.5$ AB mag. The left panel shows the panchromatic image, which has been used by SExtractor program (Bertin et al. 1996) as the source identification template. The corresponding $K - L/K$ color magnitude diagram is shown on the right.

convolved with the telescope point spread function (PSF). The spectra are then multiplied by the wavelength dependent throughput. From this spectral data cube the interferogram cube is calculated by a Fourier transform, and noise is added at each OPD step. The noise sources treated are photon shot noise (from the target, the zodiacal light, and thermal emission from the telescope), detector noise due to dark current, and read-noise. The noisy interferogram cube is then Fourier transformed back into a spectral data cube.

Fig. 6 shows the simulated data typical of ultra-deep low resolution spectrophotometry of a $4.''9 \times 4.''9$ region (0.02% of the IFIRS FOV) with input data from Im & Stockman (1998). Crowding is significant: at least 6 of the $z > 5$ galaxies lie behind the spiral, and several others are obscured by other foreground galaxies. We have added a SN Ia at the redshift of the spiral and a $z = 12$ star forming proto-cluster. The proto-cluster has $F_\nu = 2$ nJy, and has been forming stars at a rate of $2.5 M_\odot \text{ yr}^{-1}$ for 10^7 yr. In this example six broad photometric bands, *ZJHKLM*, are synthesized. The total exposure time of 10^6 s is chosen to match the ultra-deep exposure from the Galaxy Evolution DRM. The 10σ limits are 32.7 AB at K and 34.5 AB (panchromatic).

Fig. 7 shows simulated data from a 10^5 s, $R = 100$, $1 - 5 \mu\text{m}$ observation. The extracted IFIRS spectrum of the $z = 12$ proto-cluster shows $\text{Ly}\alpha$ emission, the continuum longward of the line, and the continuum break across the line due to intervening HI. The detection of emission lines allows IFIRS to measure redshifts and star formation rates. Given the large number of objects that will be simultaneously observed and the deep imaging and spectroscopy that will be available for each object, it will be possible to map out the co-evolution of the star formation and morphological evolutionary history of galaxies. All objects with $F_\nu > 0.15$ nJy are detected in the panchromatic image. The statistics of the deep image illustrate the approach to the crowding limit and the diagnostic power of panchromatic imaging: approximately 33% of the pixels in the panchromatic image have values $> 5\sigma$ above sky. The simulation illustrates the speed

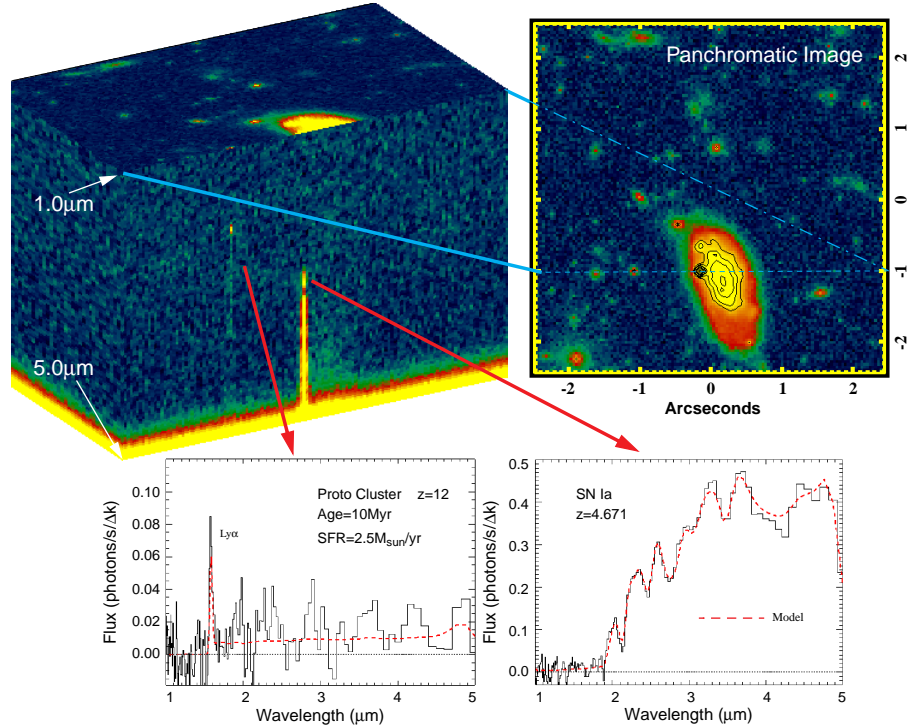


Figure 7. Simulated 10^5 s $R = 100$ $1 - 5 \mu\text{m}$ IFIRS observation. The data cube, panchromatic image, and spectral extractions are displayed. A $4.''9 \times 4.''9$ (i.e., 0.02% of the IFIRS FOV) field is shown. The input data is from Im & Stockman (1998). The data cube (top left) has been sliced open to reveal the spectra of a $z=12$ star forming proto-cluster and a SN Ia $z=4.67$ (the redshift of the spiral galaxy). The horizontal dashed line on the panchromatic image (top right), shows the where the cube is sliced. Extracted spectra are shown at the bottom along with the input model (dashed). The NEFD at $3 \mu\text{m}$ is $\simeq 3$ nJy.

with which IFIRS can implement imaging and spectroscopic surveys, the high quality data that IFIRS will produce, and the need for IFIRS's full field spectroscopic ability to spectrally and spatially separate background objects from foreground ones.

Growth of Structure & Clustering: The redshift evolution of galaxy clustering is a fundamental test of structure formation theories. The amount and form of clustering in a galaxy population can be estimated from a redshift survey (e.g., Fig. 8) using a variety of sophisticated statistical measures, the simplest of which is the two-point correlation function ξ . Formal error estimates for ξ scale as the square root of the number of galaxies in each redshift bin, so very large samples are needed. Samples of a few hundred galaxies resulting from conventional MOS surveys in a particular field will be entirely inadequate to address this problem. The need for large samples is made more extreme by the vastly extended redshift range probed by NGST and by the clear desire to subdivide any galaxy sample still further to look for clustering as a function of galaxy properties such as luminosity, color, star formation rate, or morphology

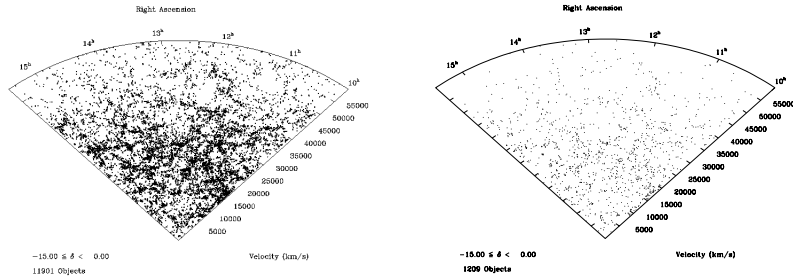


Figure 8. Two versions of a 15° slice from the Las Campanas Redshift Survey (Schectman et al. 1996). In the left hand panel all 11901 galaxies are plotted, and structure is apparent. In the right hand panel only one galaxy in ten (1209), selected at random, are plotted, and the structure is no longer apparent (M. Postman, private communication). IFIRS will produce redshifts for tens of thousands of galaxies per field over a vastly greater redshift range, rendering NGST extremely effective for studying the evolution of structure.

(cf. Kauffmann et al. 1999). For such studies, sample sizes of $\sim 10^5$ objects, much larger than estimated in the Galaxy DRM proposals, are needed and feasible with the spatial multiplexing capability of IFIRS.

Since IFIRS deep field observations produce large numbers of redshifts in a single field (1.8×1.8 Mpc at $z = 5$), isolating correlated structures (clusters, filaments, sheets) in redshift space is automatic. Hence, IFIRS will enable the investigation of various relations (e.g., morphology vs. density, star formation rate vs. density) in coherent structures and trace the evolution of these relations as a function of redshift. IFIRS surveys in the regions of rich galaxy clusters will provide ready identification of cluster members and diffuse line emission associated with the clusters, as well as the ability to identify and obtain redshifts for background lensed objects.

Fig. 9 shows that pure FTS observations are appropriate for high spectral resolution observations needed to study clustering properties. Since the sensitivity of an IFTS to an unresolved emission line is independent of spectral resolution IFIRS has sufficient sensitivity to detect emission lines ($EW \simeq 20 \text{ \AA}$) in faint ($K \simeq 29 \text{ AB}$) galaxies. This permits IFIRS to study kinematics, chemical composition, or peculiar velocities.

4. CONCLUSIONS

IFIRS enables a wide variety of NGST science, while it lends to spectroscopy the potential for serendipity that is normally accorded only to imaging. Thus, it is a powerful tool for discovery. The advantages of the IFTS concept are:

1. Deep imaging acquired simultaneously with higher spectral resolution data over a broad wavelength range.
2. “Hands-off”, unbiased, multi-object, slitless spectroscopy (ideal for moving objects). Efficient in confusion limit.
3. Flexible resolution ($R = 1 - 10,000$).
4. High throughput (near 100%) dual-port design.

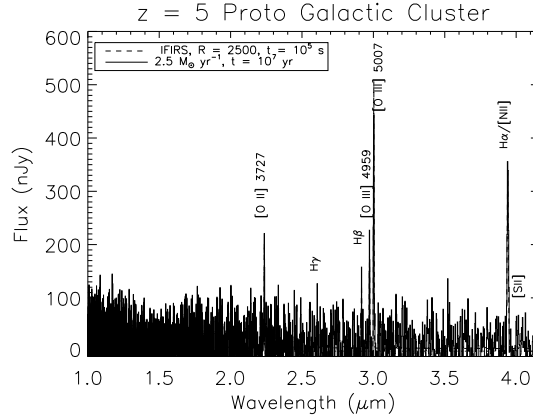


Figure 9. Simulated $R = 2500$ (pure FTS mode) observation. The target is a $K = 29.2$ AB star forming galaxy ($0.25L^*$) at $z = 5$. [O II], [O III], $H\beta$ and $H\alpha$ /[NII] are detected. The $H\beta$, [O III] $\lambda\lambda$ 4959, 5007 complex is resolved permitting measurement of the enrichment of α -process elements. The rest frame equivalent width of [OII] is 40 \AA .

5. Tolerant of cosmic rays, read-noise, dark current, and light leaks.
6. Simple and reliable calibration.
7. Proven technology with low development costs.

I am indebted to the IFIRS team for their contributions: M. Abrams, C. Bennett, J. Carr, K. Cook, A. Dey, R. Hertel, N. Macoy, S. Morris, J. Najita, A. Villemaire, E. Wishnow, & R. Wurtz. This work was support by NASA.

References

- Beer, R. 1992, Remote Sensing by Fourier Transform Spectrometry , John Wiley and Sons, New York, N. Y.
- Bennett, C. L. 2000, in Imaging the Universe in Three Dimensions. ASP Conference Series, W. van Breugel & J. Bland-Hawthorn (eds.)
- Bertin, E. & Arnouts, S. 1996, A&AS, 117, 393
- Graham, J.R. et al. 1998, PASP, 110, 1205
- Graham, J. R. 2000, in Imaging the Universe in Three Dimensions. ASP Conference Series, W. van Breugel & J. Bland-Hawthorn (eds.)
- Haiman, Z. & Loeb, A. 1998, ApJ, 503, 505
- Im, M. and Stockman, H.S. 1998, in Science with the NGST , eds., E.P. Smith and A. Koratkar, ASP Conf. Ser. vol 133, p. 263
- Kauffmann, G., Colberg, J.M., Diaferio, A., and White, S.D.M. 1999, MNRAS, 303, 188
- Shectman, S. A. et al. 1996, ApJ, 470, 172